Electronic Supplementary Material (ESI) for Physical Chemistry Chemical Physics.

Supporting Information

Transition-State Correlations for Predicting Thermochemistry of Adsorbates and Surface Reactions

Sophia J. Kurdziel[1] and Dionisios G. Vlachos[1,2]*

[1]*Department of Chemical and Biomolecular Engineering, University of Delaware, 150 Academy Street, Newark, DE 19716*

[2]*Catalysis Center for Energy Innovation, RAPID Manufacturing Institute, Delaware Energy Institute (DEI), University of Delaware, 221 Academy Street, Newark, DE 19716*

*Corresponding author: *vlachos@udel.edu*

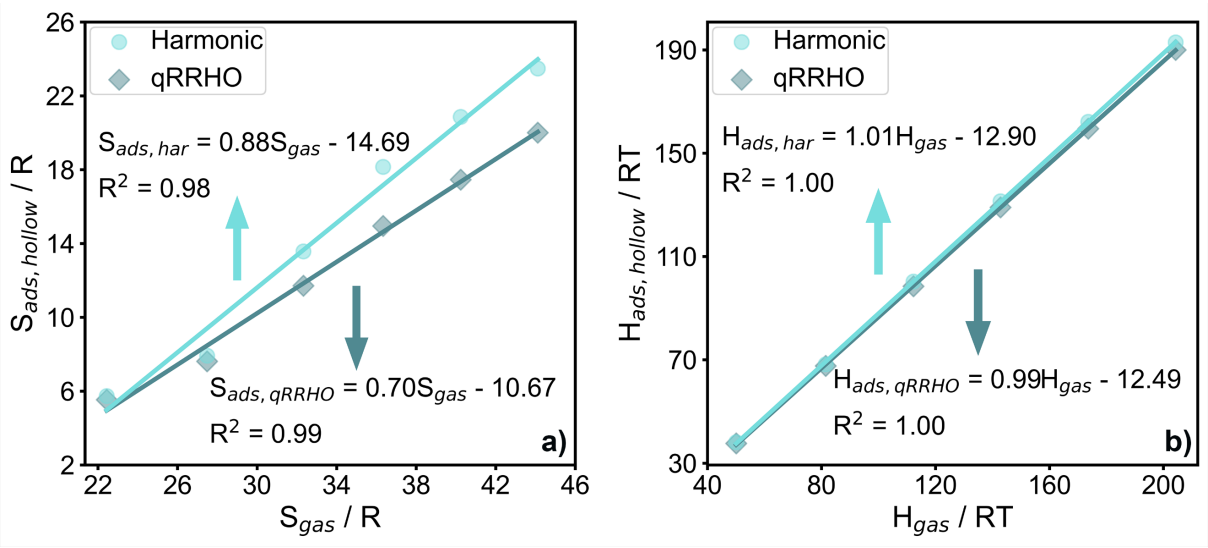

Figure S1. Thermochemical scaling for C_1-C_6 alkyl chains adsorbed in the fcc hollow site of Cu(111) (and Ni(111) for ethyl only) against gas-phase *n*-alkanes. For **a)** entropies (S_{ads}) and **b)** enthalpies (H_{ads}) thermochemistry is calculated using the harmonic approximation (circles) or the quasi-rigid rotor harmonic oscillator (qRRHO) approximation (diamonds) at 298.15 K. Slopes, y-intercepts, and fits are rounded to two decimal places for brevity. The Ni(111) surface is used for ethyl adsorption due to instability (multiple imaginary modes) of ethyl in the Cu(111) hollow site.

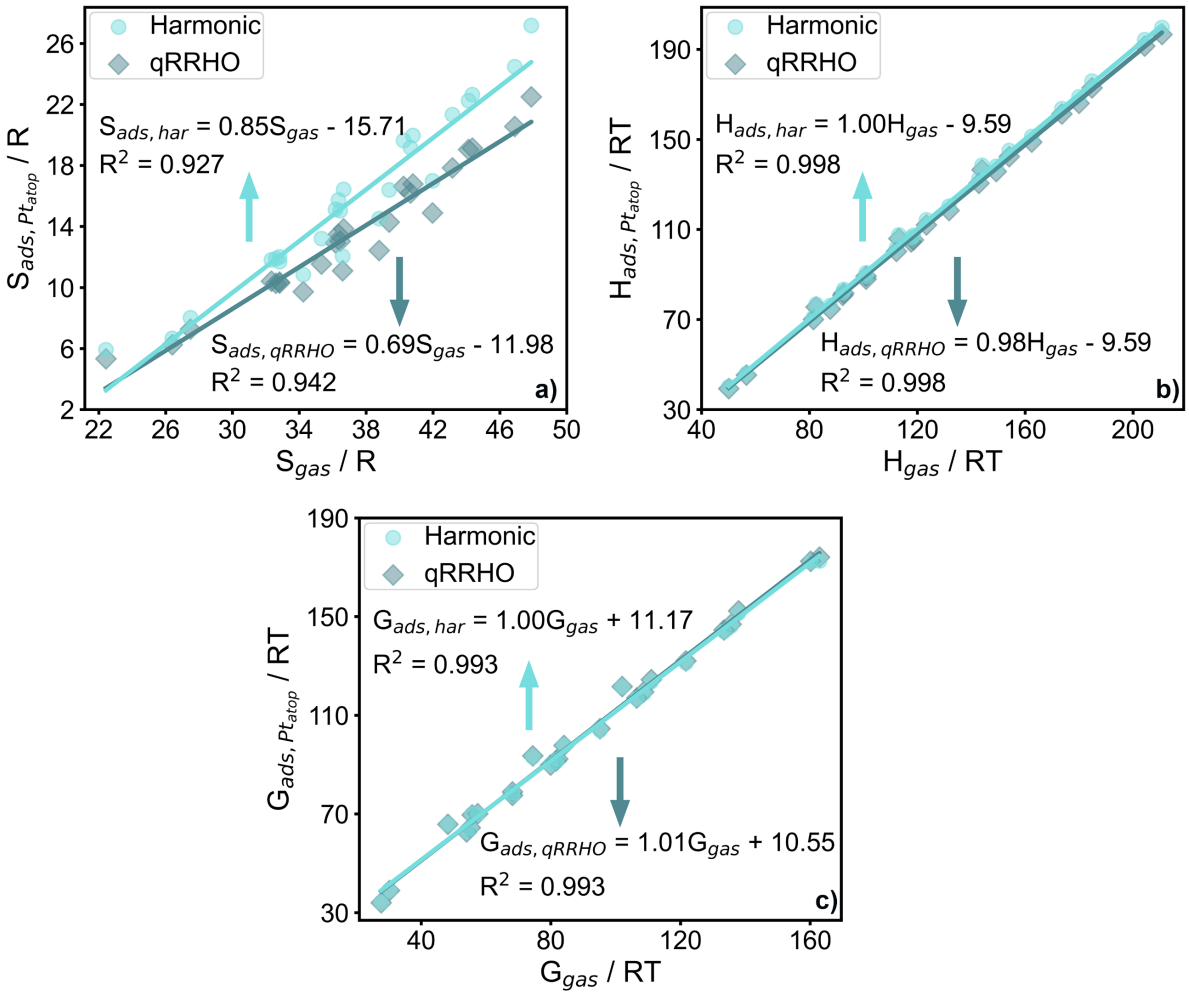

Figure S2. Thermochemical scaling for species adsorbed on the atop site of Pt(111) surfaces against gas-phase entropies. For **a)** entropies (S_{ads}), **b)** enthalpies (H_{ads}), and **c)** Gibbs energies (G_{ads}) thermochemistry is calculated using the harmonic approximation (circles) or the quasi-rigid rotor harmonic oscillator (qRRHO) approximation (diamonds) at 298.15 K.

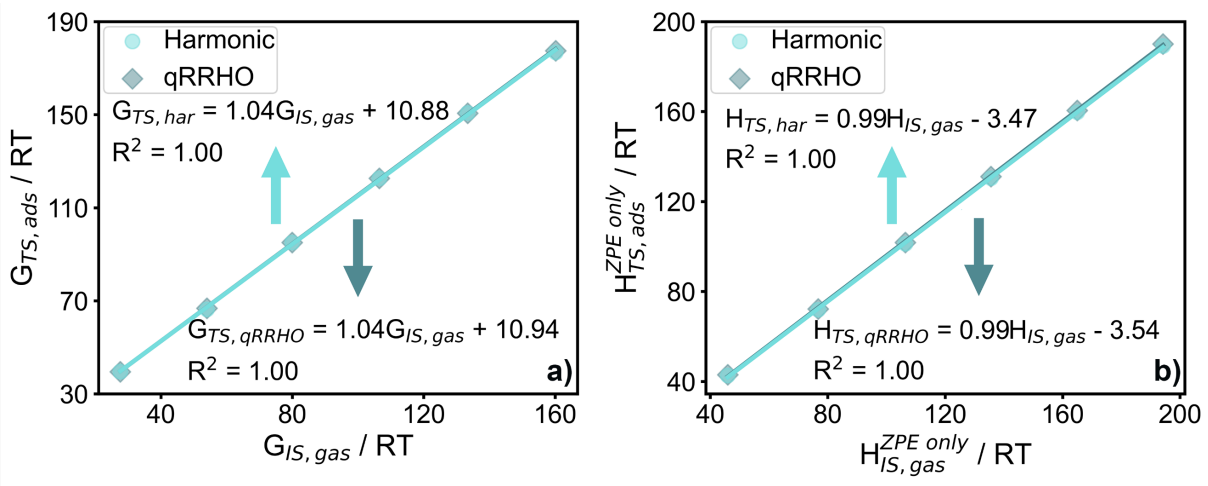

Figure S3. a) Gibbs energy scaling of transition states (TSs) with initial states (ISs) in the gas-phase for C_1-C_6 dehydrogenation reactions on Pt(111). **b)** Zero point energy (ZPE) scaling between TSs and ISs in the gas phase for the same reaction series. Harmonic (circles) and quasi-rigid rotor harmonic oscillator (diamonds) models are used; quantities calculated at 298.15 K. Slopes, y-intercepts, and fits are rounded to two decimal places for brevity.

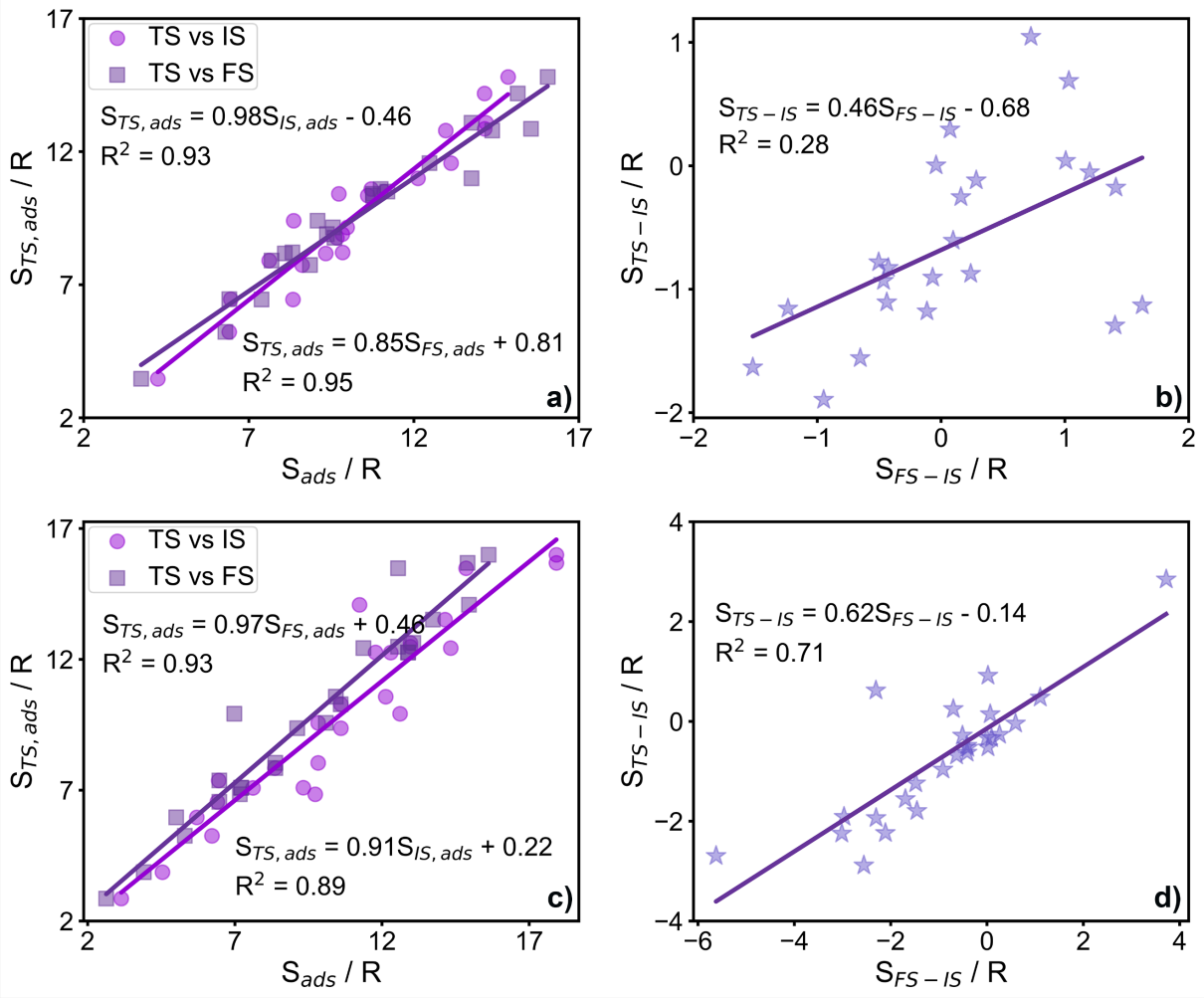

Figure S4. Entropic scaling of either initial (IS) or final (FS) states with transition (TS) states of **a)** C-C or **c)** C-H bond scissions for DFT-obtained data of propane / ethane hydrogenolysis on Ru(0001) calculated at 473.15 K. Analogous to an energy-scaling BEP relationship, for the same **b)** C-C and **d)** C-H bond scission reactions, the entropy of the transition state – initial state is plotted against the entropy of the final state – initial state.

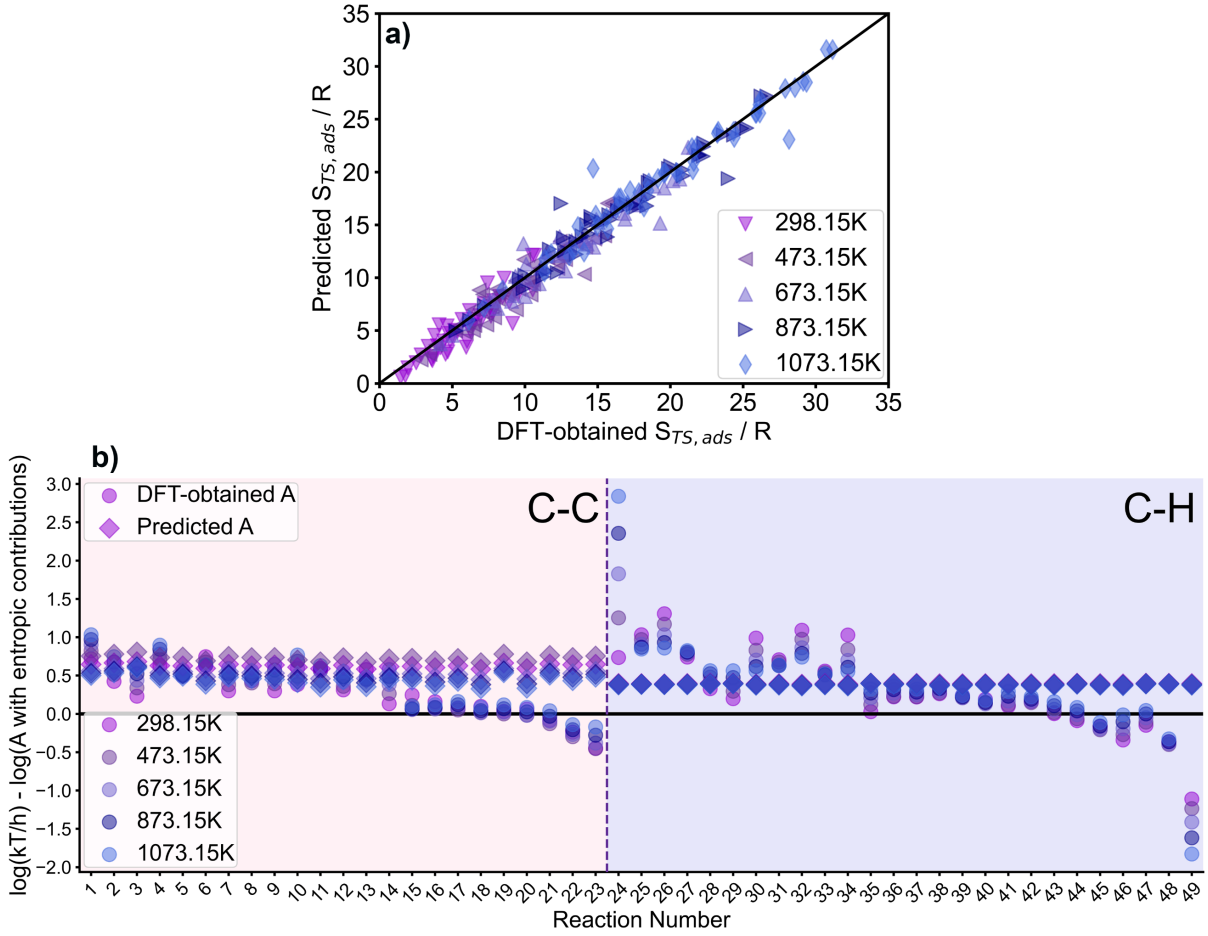

Figure S5. **a)** Parity plot of transition state entropies predicted from linear regressions in Figure 4 of the main text plotted against transition state entropies calculated from exact DFT data at varying temperatures. **b)** Difference between the log of $\frac{k_b T}{h}$ and the log of the pre-exponential (A) computed using entropic contributions either obtained from exact DFT data or from the linear regressions in Figure 4 of the main text. The reactions are numbered arbitrarily as integers except to distinguish between C-C and C-H reactions; reactions 1-23 are C-C bond scissions and reactions 24-49 are C-H bond scissions. Pre-exponentials are in units of s^{-1}.

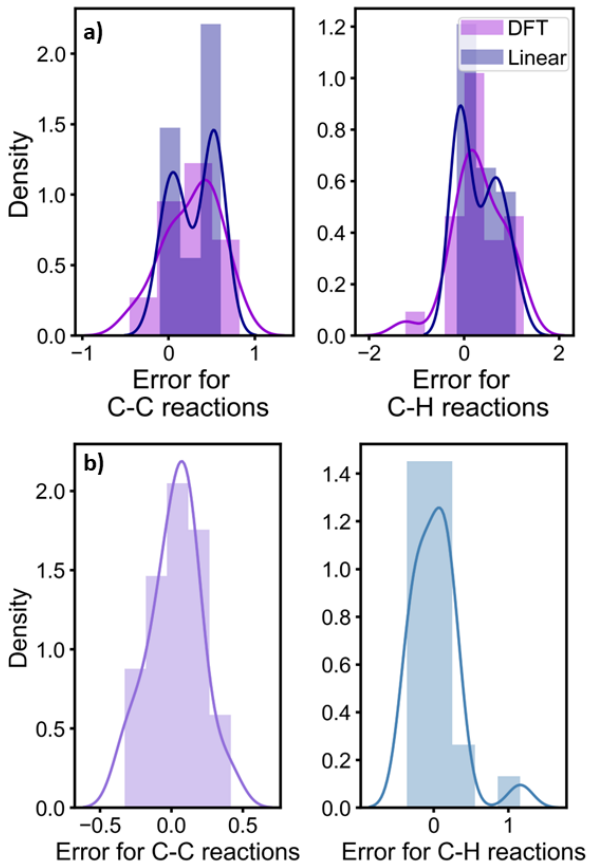

Figure S6. **a)** Distribution of errors between the log of $\frac{k_b T}{h}$ and the log of the pre-exponential computed using entropic contributions either obtained from exact DFT data or from linear regressions for C-C and C-H bond scission steps. **b)** Distribution of errors between the log of the pre-exponential calculated from exact DFT data minus that calculated from linear regressions for C-C and C-H bond scission steps. Pre-exponentials computed at 473.15 K. Pre-exponentials are in units of s^{-1}.

Table S1. Gas-phase / adsorbate entropies calculated at 298.15 K using the quasi-rigid rotor harmonic oscillator (qRRHO) or harmonic oscillator (HO) models on fcc(111) surface sites. (##) Denotes if 1 small imaginary mode (< 50*i* cm^{-1}) was present and replaced with 20 cm^{-1}.

Gas-Phase Species	S_{gas} / R	Adsorbate	Surface / Adsorption Site	S_{ads} / R HO	S_{ads} / R qRRHO
CH_4	22.43	CH_3^*	Pt / atop	5.92	5.33
C_2H_6	27.48	$C_2H_5^*$	Pt / atop	8.02	7.27
C_3H_8	32.33	$C_3H_7^*$	Pt / atop	11.81	10.41
C_4H_{10}	36.34	$C_4H_9^*$	Pt / atop	15.74	13.50
C_5H_{12}	40.24	$C_5H_{11}^*$	Pt / atop	19.64	16.62
C_6H_{14}	44.12	$C_6H_{13}^*$ ##	Pt / atop	22.25	19.05
CH_4	22.43	CH_3^*	Rh / atop	5.89	5.43
C_2H_6	27.48	$C_2H_5^*$	Rh / atop	8.74	7.79
C_3H_8	32.33	$C_3H_7^*$	Rh / atop	11.69	10.56
C_4H_{10}	36.34	$C_4H_9^*$	Rh / atop	15.90	13.76
C_5H_{12}	40.24	$C_5H_{11}^*$	Rh / atop	18.52	16.27
C_6H_{14}	44.12	$C_6H_{13}^*$	Rh / atop	22.75	19.49
CH_4	22.43	CH_3^*	Cu / fcc	5.74	5.53
C_2H_6	27.48	$C_2H_5^*$	Ni / fcc	7.92	7.61
C_3H_8	32.33	$C_3H_7^*$	Cu / fcc	13.57	11.71
C_4H_{10}	36.34	$C_4H_9^*$ ##	Cu / fcc	18.15	14.95
C_5H_{12}	40.24	$C_5H_{11}^*$	Cu / fcc	20.86	17.45
C_6H_{14}	44.12	$C_6H_{13}^*$ ##	Cu / fcc	23.48	20.00
C_2H_5OH	32.59	$C_2H_5O^*$	Pt / atop	11.90	10.27
C_3H_7OH	36.44	$C_3H_7O^*$	Pt / atop	15.04	13.04
C_4H_9OH	40.65	$C_4H_9O^*$	Pt / atop	19.16	16.20
$C_5H_{11}OH$	44.35	$C_5H_{11}O^*$	Pt / atop	22.65	19.14
$C_6H_{13}OH$	47.88	$C_6H_{13}O^*$ ##	Pt / atop	27.18	22.51
C_3H_6O	35.32	$C_3H_5O^*$	Pt / atop	13.20	11.54
C_4H_8O	39.37	$C_4H_7O^*$	Pt / atop	16.40	14.28
$C_5H_{10}O$	43.16	$C_5H_9O^*$	Pt / atop	21.33	17.84
$C_6H_{12}O$	46.89	$C_6H_{11}O^*$	Pt / atop	24.48	20.56
$(CH_3)_2CHOH$	36.16	$(CH_3)_2CHO^*$	Pt / atop	15.12	12.92
$(CH_3)_2CO$	36.59	$CH_3COCH_2^*$	Pt / atop	12.05	11.10
C_2H_4	26.40	$C_2H_3^*$	Pt / atop	6.67	6.25
C_3H_6	34.24	$C_3H_5^*$	Pt / atop	10.85	9.72
C_4H_8	38.78	$C_4H_7^*$	Pt / atop	14.52	12.43
C_5H_{10}	41.97	$C_5H_9^*$	Pt / atop	16.99	14.89
$C_2H_5NH_2$	32.82	$C_2H_5NH^*$	Pt / atop	11.70	10.36
$C_2H_5NH_2$	32.82	$C_2H_4NH_2^*$	Pt / atop	12.01	10.29

$C_3H_7NH_2$	36.65	$C_3H_7NH^*$	Pt / atop	16.43	13.84
$C_4H_9NH_2$	40.79	$C_4H_9NH^*$ ##	Pt / atop	19.96	16.79

Table S2. Gas-phase / adsorbate enthalpic corrections calculated at 298.15 K using the quasi-rigid rotor harmonic oscillator (qRRHO) or harmonic oscillator (HO) models on fcc(111) surface sites. (##) Denotes if 1 small imaginary mode (< 50*i* cm^{-1}) was present and replaced with 20 cm^{-1}.

Gas-Phase Species	H_{gas} / RT	Adsorbate	Surface / Adsorption Site	H_{ads} / RT HO	H_{ads} / RT qRRHO
CH_4	50.08	CH_3^*	Pt / atop	40.14	39.33
C_2H_6	81.48	$C_2H_5^*$	Pt / atop	70.95	70.01
C_3H_8	112.26	$C_3H_7^*$	Pt / atop	101.76	100.28
C_4H_{10}	142.82	$C_4H_9^*$	Pt / atop	132.54	130.54
C_5H_{12}	173.64	$C_5H_{11}^*$	Pt / atop	163.66	161.27
C_6H_{14}	204.29	$C_6H_{13}^*$ ##	Pt / atop	194.34	191.48
CH_4	50.08	CH_3^*	Rh / atop	39.23	38.50
C_2H_6	81.48	$C_2H_5^*$	Rh / atop	70.04	68.93
C_3H_8	112.26	$C_3H_7^*$	Rh / atop	100.88	99.43
C_4H_{10}	142.82	$C_4H_9^*$	Rh / atop	131.52	129.64
C_5H_{12}	173.64	$C_5H_{11}^*$	Rh / atop	162.55	160.27
C_6H_{14}	204.29	$C_6H_{13}^*$	Rh / atop	193.25	190.55
CH_4	50.08	CH_3^*	Cu / fcc	38.11	37.63
C_2H_6	81.48	$C_2H_5^*$	Ni / fcc	68.29	67.66
C_3H_8	112.26	$C_3H_7^*$	Cu / fcc	100.32	98.47
C_4H_{10}	142.82	$C_4H_9^*$ ##	Cu / fcc	131.39	128.99
C_5H_{12}	173.64	$C_5H_{11}^*$	Cu / fcc	162.12	159.46
C_6H_{14}	204.29	$C_6H_{13}^*$ ##	Cu / fcc	192.89	189.97
C_2H_5OH	87.70	$C_2H_5O^*$	Pt / atop	76.16	74.66
C_3H_7OH	118.57	$C_3H_7O^*$	Pt / atop	107.30	105.34
C_4H_9OH	149.27	$C_4H_9O^*$	Pt / atop	138.06	135.71
$C_5H_{11}OH$	179.97	$C_5H_{11}O^*$	Pt / atop	168.90	166.09
$C_6H_{13}OH$	210.74	$C_6H_{13}O^*$ ##	Pt / atop	199.74	196.62
C_3H_6O	92.72	$C_3H_5O^*$	Pt / atop	83.34	81.62
C_4H_8O	123.39	$C_4H_7O^*$	Pt / atop	114.25	112.07
$C_5H_{10}O$	154.11	$C_5H_9O^*$	Pt / atop	145.05	142.34
$C_6H_{12}O$	184.79	$C_6H_{11}O^*$	Pt / atop	175.94	172.91
$(CH_3)_2CHOH$	117.72	$(CH_3)_2CHO^*$	Pt / atop	106.31	104.46
$(CH_3)_2CO$	92.31	$CH_3COCH_2^*$	Pt / atop	82.02	80.69
C_2H_4	56.62	$C_2H_3^*$	Pt / atop	45.97	45.27
C_3H_6	82.48	$C_3H_5^*$	Pt / atop	76.77	75.52

C_4H_8	113.18	$C_4H_7^*$	Pt / atop	107.59	105.96
C_5H_{10}	143.97	$C_5H_9^*$	Pt / atop	138.49	136.54
$C_2H_5NH_2$	101.00	$C_2H_5NH^*$	Pt / atop	89.36	87.91
$C_2H_5NH_2$	101.00	$C_2H_4NH_2^*$	Pt / atop	90.74	89.27
$C_3H_7NH_2$	131.79	$C_3H_7NH^*$	Pt / atop	120.36	118.44
$C_4H_9NH_2$	162.46	$C_4H_9NH^*$ ##	Pt / atop	151.26	148.82

Table S3. The percent contribution of partitional components to the total gas-phase entropy for propane and hexane.

Partition Function	Molecule	Percent contribution to total entropy
Vibrational	Propane	8.7%
	Hexane	25.6%
Translational	Propane	58.1%
	Hexane	44.8%
Rotational	Propane	33.2%
	Hexane	29.6%

Table S4. DFT-obtained data for listed reactions in propane and ethane hydrogenolysis on Ru(0001) used for constructing Figures 4 and 5 in the main text.

Elementary reaction steps used for DFT-derived scaling relations	
C-C Bond Scission	**C-H Bond Scission**
CC* + * ⇄ C* + C*	CH* + * ⇄ C* + H*
$CCCH_2$* + * ⇄ C* + CCH_2*	CHC* + * ⇄ CC* + H*
CHCC* + * ⇄ CH* + CC*	CH_2* + * ⇄ CH* + H*
CHCH* + * ⇄ CH* + CH*	CH_2C* + * ⇄ CHC* + H*
CH_2C* + * ⇄ CH_2* + C*	CH_3* + * ⇄ CH_2* + H*
CH_2CCH_2* + * ⇄ CH_2* + CCH_2*	CH_3C* + * ⇄ CH_2C* + H*
CH_2CH_2* + * ⇄ CH_2* + CH_2*	CH_3CCH* + * ⇄ CH_2CCH* + H*
CH_2CH* + * ⇄ CH_2* + CH*	CH_3CH_2* + * ⇄ CH_2CH_2* + H*
CH_2CCH* + * ⇄ CH_2C*+ CH*	CH_3CH* + * ⇄ CH_2CH* + H*
CH_2CHCH* + * ⇄ CH_2CH* + CH*	CH_2CH* + * ⇄ CH_2C* + H*
CH_3C* + * ⇄ CH_3* + C*	CH_2CH_2* + * ⇄ CH_2CH* + H*
CH_3CCH_3* + * ⇄ CH_3* + CCH_3*	CH_4* + * ⇄ CH_3* + H*
CH_3CH_2* + * ⇄ CH_3* + CH_2*	CH_3CH* + * ⇄ CH_3C* + H*
CH_3CH* + * ⇄ CH_3* + CH*	CH_3CCH_2* + * ⇄ CH_3CCH* + H*
CH_3CHCH_3* + * ⇄ CH_3* + $CHCH_3$*	CH_3CH_2* + * ⇄ CH_3CH* + H*
CH_3CC* + * ⇄ CH_3C* + C*	$CH_3CH_2CH_2$* + * ⇄ CH_3CHCH_2* + H*
CH_3CCH* + * ⇄ CH_3C* + CH*	$CH_3CH_2CH_3$* + * ⇄ CH_3CHCH_3* + H*
CH_3CHCH_2* + * ⇄ CH_3CH* + CH_2*	CH_3CH_3* + * ⇄ CH_3CH_2* + H*
CH_3CH_2C* + * ⇄ CH_3CH_2* + C*	$CH_3CH_2CH_2$* + * ⇄ CH_3CH_2CH* + H*
$CH_3CH_2CH_2$* + * ⇄ CH_3CH_2* + CH_2*	$CH_3CH_2CH_3$* + * ⇄ $CH_3CH_2CH_2$* + H*

$CH_3CH_2CH^* + * \rightleftarrows CH_3CH_2^* + CH^*$ $CHCCH^* + * \rightleftarrows CHC^* + CH^*$ $CHCHCH^* + * \rightleftarrows CHCH^* + CH^*$	$CH_2CHCH_2^* + * \rightleftarrows CH_2CHCH^* + H^*$ $CH_3CHCH_3^* + * \rightleftarrows CH_3CHCH_2^* + H^*$ $CHCH^* + * \rightleftarrows CHC^* + H^*$ $CH_2CH^* + * \rightleftarrows CHCH^* + H^*$ $CH_2CHCH_2^* + * \rightleftarrows CH_2CCH_2^* + H^*$ $CH_3CHCH^* + * \rightleftarrows CH_3CCH^* + H^*$

Supplementary Note S1 – Justification of Linearity for Entropic Contributors

Equations S1-S3 are first-order Taylor series expansions of each entropic contributor, where the Taylor series expansions demonstrate whether entropic contributions as a function of size may be approximated as linear or not. The translational entropy is linearized around a reference molar mass (m_o), the rotational entropy around a reference rotational moment of inertia ($(I_A I_B I_C)_o$), and the vibrational entropy around a reference frequency (ν_o):

$$\frac{S_{trans}}{R} = \left(\frac{3}{2} ln\left(\frac{2\pi m_o}{h^2}\right) + \frac{5}{2} ln(k_B T) - ln(p) + \frac{5}{2}\right) + \left(\frac{3R}{2m_o}\right)(m - m_o), \quad \text{S1}$$

$$\frac{S_{rot}}{R} = \left(ln\left(\frac{8\pi^2}{\sigma}\right) + \frac{3}{2} ln\left(\frac{2\pi k_B T}{h^2}\right) + \left(\frac{1}{2} ln(I_A I_B I_C)_o\right) + \frac{3}{2}\right) + \left(\frac{R}{2(I_A I_B I_C)_o}\right)\left((I_A I_B I_C) - (I_A I_B I_C)_o\right), \quad \text{S2}$$

$$\frac{S_{vib}}{R} = \frac{h\nu_o}{T\left(e^{\frac{h\nu_o}{k_B T}} - 1\right)} + \left[\frac{h\left(e^{\frac{h\nu_o}{k_B T}} - 1 - \left(\frac{h\nu_o}{k_B T} e^{\frac{h\nu_o}{k_B T}}\right)\right)}{T\left(e^{\frac{h\nu_o}{k_B T}} - 1\right)^2}\right](\nu_i - \nu_o)$$
$$-k_B ln\left(1 - e^{\frac{-h\nu_o}{k_B T}}\right) - \left[\frac{h}{T\left(e^{\frac{h\nu_o}{k_B T}} - 1\right)}\right](\nu_i - \nu_o). \quad \text{S3}$$

The rotational entropy also contains the symmetry number σ, but this term is unrelated to the size of the molecule, so it is taken as a constant in the Taylor series expansion. Figure S7 shows parity plots of the Taylor expansion against the calculated entropic component. For the translational and rotational entropies, deviations from the true value using the Taylor expansion indicate the nonlinear nature of the mass-dependent component. For translational entropy (Figure S7a), there is a logarithmic dependence on the molar mass, although in a given range or tolerance, the relation could be approximated as linear. For rotational entropy (Figure S7b), the logarithmic nature of the curve plotted against molar mass comes from dependence on the moment of inertia. The rotational motions characterized by moments of inertia for polyatomic molecules are determined from components of the inertial tensor, which contains elements directly dependent on the mass and coordinates of atoms. The vibrational entropy successively increases for the C_1-C_6 alkane \ alkyl homologous series as the vibrational degrees of freedom increase. The Taylor series expansion around a reference frequency validates how individual vibrational frequencies are linearly correlated between molecules of different sizes, thus establishing the linearity of thermochemical scaling relationships. Figure S7c and S7d demonstrate this; vibrational entropies calculated for individual frequencies for c) butane and d) butyl are linearized around a corresponding frequency from c) propane and

d) propyl. The reference frequencies are determined using a rolling correlation, which measures the correlation between two series on a rolling window. Pearson correlation coefficients are calculated from rolling correlations where all possible individual entropic configurations are mapped from a larger to a smaller array. The highest coefficient is taken, and the frequencies in this pairing are used for the Taylor expansion.

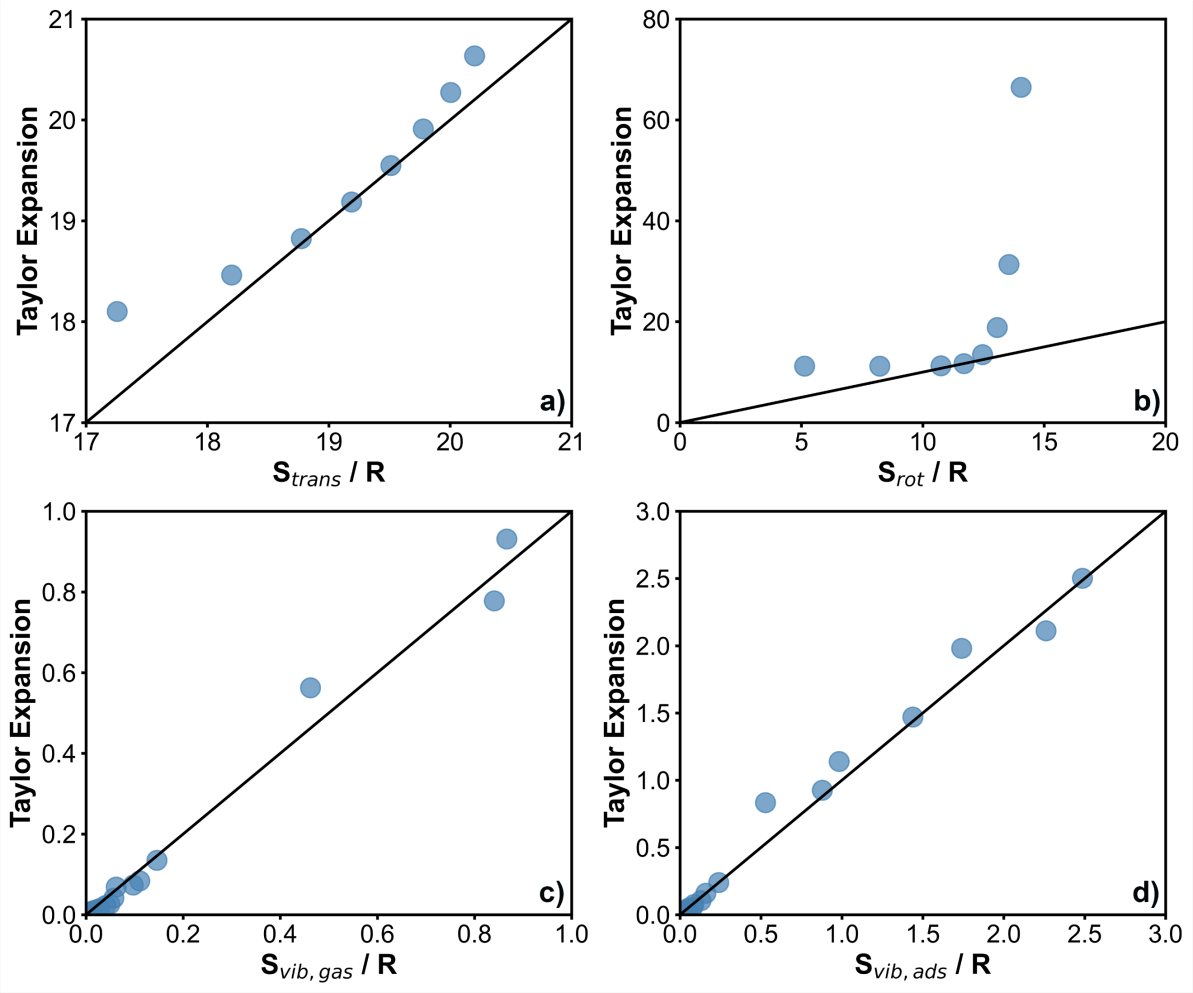

Figure S7. First-order Taylor series expansion plotted against **a)** translational, **b)** rotational entropic components for C_1-C_8 alkanes (gas phase). Vibrational entropies calculated for individual frequencies for **c)** butane and **d)** butyl are linearized around a corresponding frequency from **c)** propane and **d)** propyl. Adsorbed vibrational components are calculated from the Pt(111) surface. The black line indicates parity. Quantities calculated at 298.15 K.